

# Multimodal Functional and Morphological Nonrigid Image Registration

Rui Bernardes, Pedro Baptista and José Cunha-Vaz

Center of New Technologies for Medicine  
Assoc. for Innovation and Biomedical Research on Light and Image  
Coimbra, Portugal

Jorge Dias

Departamento de Engenharia Electrotécnica e de Computadores  
Universidade de Coimbra  
Coimbra, Portugal

José Cunha-Vaz  
Faculdade de Medicina  
Universidade de Coimbra  
Coimbra, Portugal

**Abstract**—The aim of this work is to present the registration of two different and complementary imaging modalities of the human eye fundus. One is a widely used modality consisting of a color photograph of the human retina and the other consists of a functional imaging modality that assesses, *in vivo*, the human blood–retinal barrier function. The need for the nonrigid registration of these two modalities is demonstrated and is due to the acquisition mode of the functional modality.

The two modalities herewith registered are from two different devices, have different resolutions and different fields-of-view, i.e., the smaller is only a subset of the larger one. In this paper, all these problems were addressed and a solution proposed.

## I. INTRODUCTION

The fusion of functional and morphological information from *in vivo* imaging modalities of the human eye fundus is a major need both on the assessment of treatment efficacy, e.g., drug efficacy, and on the monitoring of disease progression on the initial stages of diabetic retinopathy. One widely used modality consists in a color photograph of the eye fundus, the so called retinography, that documents the visible changes both on morphology and on the color contents of the eye fundus. It also serves as a fundus reference on a per-eye basis. The other modality used in this work consists in the functional imaging of the human blood–retinal barrier (BRB), i.e., on the assessment of the BRB permeability to sodium fluorescein (NaFl). For details on this modality see [1]. The clinical interest on the BRB functional assessment has been already demonstrated using a previously available confocal scanning laser ophthalmoscope [2], [3], [4], [5]. Key aspects of these modalities with implication on the approach to be followed are: the region-of-interest of the eye fundus; resolution; field-of-view, and; mode of acquisition. The region-of-interest, due to the potential threat to vision, is the macular area, i.e., the area centered on the fovea and about 20° on the eye fundus.

This work was developed under the POSI/SRI/45151/2002 project, funded by the Portuguese *Fundação para a Ciência e a Tecnologia (FCT)* agency.

Due to the importance for vision, both modalities herewith considered are taken centered on the fovea and are of 50° and 20°, respectively the retinography and the BRB functional image.

## II. METHODS

The retinography modality herewith considered, consists in a digitally taken RGB color fundus photograph, 50° field-of-view, centered on the fovea and with a resolution of 768 × 576 pixels. This image is taken by a 3CCD camera mounted on a Zeiss Fundus Camera system, model FF450. On the other hand, the BRB functional image, also known as the retinal leakage analyzer (RLA), is obtained from a stack of 32 confocal planes, each one read in a raster-scan mode by an Heidelberg Retina Angiograph (HRA). Due to this raster-scan mode of acquisition and the 1.6 seconds acquisition time, where saccadic eye movements, both voluntary (e.g., when the eyes move from one fixation point to another as in reading) and non-voluntary (e.g., due to following the flying spot that illuminates the eye fundus) might occur, it is expectable that a rigid registration may not produce results with the required accuracy. The image resolution for this modality is limited to 256 × 256 pixels (maximum). For this purpose, a three-step approach was taken consisting of: A. rigid registration; B. perspective registration, and; C. nonrigid registration.

### A. Rigid Registration

The only major reference common to both modalities is the fovea. In order to extract the morphological information from the RGB color fundus photograph, a principal component analysis (PCA) is performed using each of the RGB channels as an independent variable. As a final result, a single monochromatic image is obtained that represents the morphology on a higher contrast image where details belonging to each channel are present. This PCA image will then be used for



Fig. 1. Color fundus photograph (retinography) with vessel centerlines in blue and candidate vessel intersections in green.

the registration procedure as it has a pixel-to-pixel relation to the original RGB image. For the RLA modality, two types of information are obtained simultaneously with a one-to-one pixel relation: a high-speed fluorescein angiography (SLO.FA) and the functional map of the BRB (color coded). While the latter contains functional information, the former image contains the morphological information necessary to be correlated to the former modality. The location of the fovea is determined by computing the cross-correlation of each modality with an inverted Gaussian (1), whose parameters were experimentally determined based on previous existing knowledge ( $\sigma$  is equal to half of the optic disc diameter).

$$g(i, j) = k \left[ 1 - \frac{1}{2} \exp \left( \frac{-(i^2 + j^2)}{2\sigma^2} \right) \right] \quad (1)$$

For vascular tree segmentation, a differential geometric approach was taken by considering the vessels as the ridges (gorges) of a 3D map, where the height is given by the intensity values of the images representing each modality. Therefore, a surface  $S = \{x, y, \mathbf{I}(x, y)\}$  is considered and the Hessian matrix computed at each pixel ( $\mathbf{H}(x_0, y_0)$ ). Being  $\mathbf{u}$  the eigenvector associated to the maximum (minimum) eigenvalue of  $\mathbf{H}(x_0, y_0)$ , the pixel at  $(x_0, y_0)$  is a ridge (gorge) if the first directional derivative across the direction  $\mathbf{u}$  at  $(x_0, y_0)$  is null [6], i.e.,

$$\langle \nabla \mathbf{I}(x_0, y_0), \mathbf{u} \rangle = 0 \quad (2)$$

Vessel centerlines are then computed by determining the skeleton of the newly computed binary images, after the application of morphological filters — erosion, dilation, skeleton and pruning (Fig. 1).

While the translational part of the rigid registration is given by the location of the fovea in each of the images, the rotation is determined by computing the translation, on the polar representation of the vascular tree, using a robust phase-correlation approach [7]. These steps allow for the rigid registration of the aforementioned modalities by computing

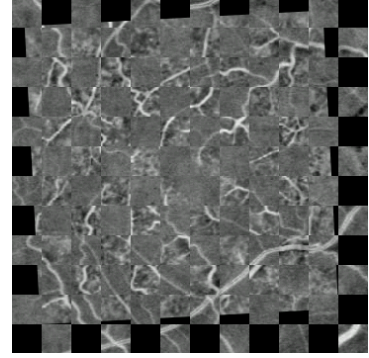


Fig. 2. Black-and-white chessboard-like representation of the rigid registration of the high-speed fluorescein angiography against the fundus reference (retinography). Only the common part is shown. Please note the difference in detail between both modalities

the location of the fovea at each modality and the rotation between these modalities (Fig. 2).

### B. Perspective registration

In the previous step, the vessel's centerlines were determined. In order to compute the location of vessel bifurcations/crossings, each binary image containing the vessel centerlines is cross-correlated with a unit matrix ( $\mathbf{J}_3$ ). Any location where the cross-correlation is over 3 is earmarked as a candidate location. This procedure is run on each modality. Using rigid registration, it is possible to remove outliers by eliminating hypothetical bifurcation locations without counterparts on the other modality. Afterwards, a modified version of the procedure established in [8] is implemented making it possible to compute the perspective transformation using the Moore-Penrose pseudo-inverse matrix, being the transformation matrix of the type:

$$\mathbf{P} = \begin{bmatrix} p_{11} & p_{12} & p_{13} \\ p_{21} & p_{22} & p_{23} \\ p_{31} & p_{32} & 1 \end{bmatrix}$$

It is important to note that for this process to be useful, one must check for an even distribution of candidates (bifurcations/crossings) over the image. Nevertheless, even more important is to have candidates close to the limits of the image. Failing this, the registration produced may be worse than the one achieved with the rigid approach. Therefore, the input to the next step may be either the rigid or the perspective approach.

### C. Nonrigid Spline-based Registration

For this final step, the RLA morphological image is considered as a set of overlapping windows ( $W$ ) of size  $M \times M$

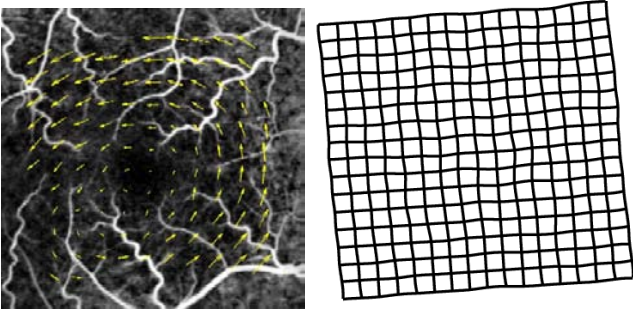


Fig. 3. Total displacement vector field (scaled for better clarity), on the left, and respective grid deformation, on the right.

centered on pixel  $(x_i, y_i)$ . This pixel on the retinography will have the coordinates  $(x_f, y_f)$  given by:

$$X_f = \mathbf{P}X_i \quad (3)$$

where  $X_i = [x_i, y_i, 1]^T$  and  $X_f = [x_f, y_f, 1]^T$  are the homogeneous coordinates on the SLO.FA and retinography, respectively, and  $\mathbf{P}$  is the 3x3 rigid/perspective transformation matrix computed in the previous steps. For the current nonrigid registration, the search area to find the best-fit for each of the  $W$  windows depends on the approach followed (rigid/perspective), being larger if the rigid approach is used. Considering the differences in image details between these modalities, the search for the best match is based on the measure of similarity yielded by the partitioned intensity uniformity (PIU) given by (4)

$$PIU_A = \sum_b \frac{n_b}{N} \frac{\sigma_A(b)}{\mu_A(b)} \quad (4)$$

where:

$$\begin{aligned} n_b &= \sum_{\Omega_a^T} 1 \\ \mu_A(b) &= \frac{1}{n_b} \sum_{\Omega_b^T} \mathbf{A}(x_A) \\ \sigma_A(b) &= \frac{1}{n_b} \sum_{\Omega_b^T} (\mathbf{A}(x_A) - \mu_A(b))^2 \end{aligned}$$

with  $\mathbf{A}(x_A)$  being the intensity of modality  $\mathbf{A}$  at coordinates  $x_A$ , and,  $\sigma_A(b)$  and  $\mu_A(b)$  respectively the variance and average of the intensity of modality  $\mathbf{A}$  at coordinates having intensities  $b$  at modality  $\mathbf{B}$ . For details see [9].

This procedure allows the determination of the vector field that indicates the displacement of each window  $W$  relatively to its position after the rigid/perspective registration. In this way, the perspective registration's role is to tighten the search area for the PIU process, thus reducing the run time necessary for the entire process. Since each modality is centered on the fovea, where there are no vessels, erratic displacement vectors, both on strength and direction, appear in this area. To overcome this problem, each displacement vector is checked for

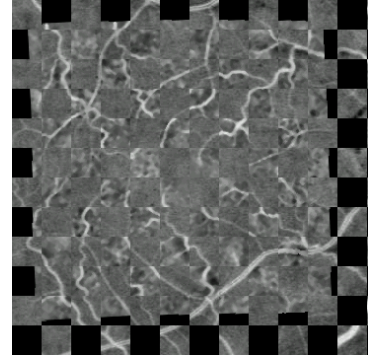


Fig. 4. Registration correcting local deformations.

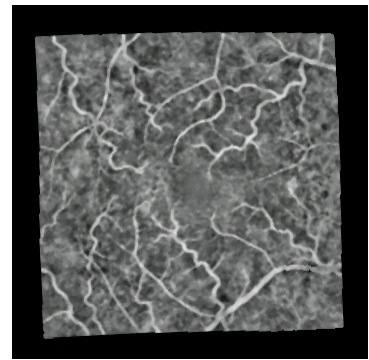


Fig. 5. Final result: fluorescein angiography part.

its direction and strength against its neighborhood to remove outliers. The final vector field is generated by a bicubic spline interpolation function fitting a surface to the displacements, on the  $x$  and  $y$  axis, where they were computed for each  $W$  window. The final vector field can be seen on Fig. 3 (left) along with the respective grid deformation (right).

The chessboard figure showing the achieved registration is shown on Fig. 4. The final registration of the fluorescein angiography part of the BRB functional imaging is shown on Fig. 5, while the same transformation on the leakage map (functional information) is shown on Fig. 6 on the following page.

The retinography overlaid with the leakage map (functional information) is shown on Fig. 7, also on the next page.

### III. RESULTS AND CONCLUSIONS

For the first time, it was possible to register the BRB functional imaging of the human eye to a color fundus photograph of the same eye in a fully automated way. It is important to note not only the multimodality involved, but also the differences in resolution, field-of-view, and the inclusion of an area with low level of morphological information from the signal's point-of-view.

An attempt to evaluate the accuracy of the three-step approach for the registration procedure was undertaken. There are several methodologies for the assessment of image registration

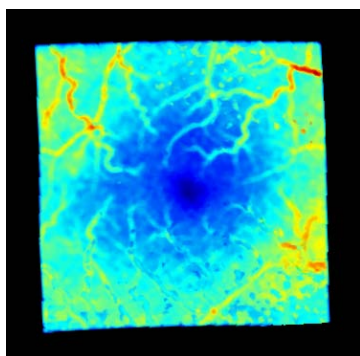


Fig. 6. Final result: leakage map (functional information) part.

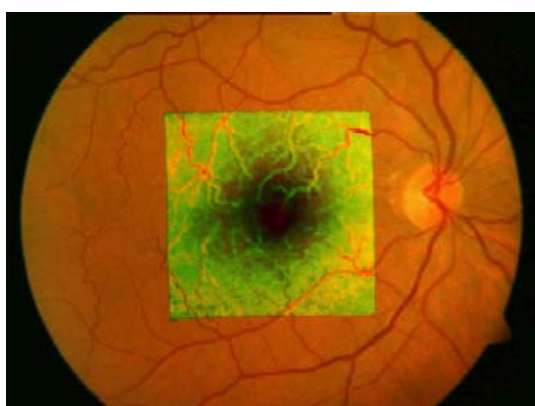


Fig. 7. Color fundus photograph (retinography) overlaid with the leakage map (functional information).

accuracy, which are reported in detail in [10]. However, since the effect of the deformation modelled by the nonrigid spline-based registration step is not easily quantifiable, and since the localization and matching errors described in [10] are not adequate (the control points used are a result of automatic detection of features, and are as such less than useful as ground truth), this assessment was attained through simple visual inspection and alignment quality evaluation alone.

More specifically, to perform the appraisal of the latter, the similarity measures described on subsection II-C, namely the PIU and correlation values for comparison between common areas of the registered images, were computed for each of the three steps of the registration process. Since these values increase as the complexity of the transformation multiplies, it can be inferred that registration accuracy improves throughout the whole process.

As has already been said, as the use of confocal scanning laser ophthalmoscopes becomes more commonplace, intrinsic image distortions due to saccadic eye movements must be taken into account when registering images acquired with these devices. The accuracy evaluation described above seems to indicate that the registration procedure presented herewith successfully deals with this problem.

This procedure will in the future be adapted for the inclusion

of other modalities, e.g., perfusion measurements, multifocal electroretinography (mfERG), etc. The fusion of complementary information on a clinical practice basis, opens new perspectives for the understanding of the changes occurring in the macular area of the human eye, thus improving our knowledge on the retinal changes occurring in health and disease.

## REFERENCES

- [1] Rui Bernardes, Jorge Dias, and José Cunha-Vaz, "Mapping the human blood-retinal barrier function," *IEEE Transactions on Biomedical Engineering*, vol. 52, no. 1, pp. 106–116, January 2005.
- [2] Conceição Lobo, Rui Bernardes, Fernando Santos, and José Cunha-Vaz, "Mapping retinal fluorescein leakage with confocal scanning laser fluorometry of the human vitreous," *Arch Ophthalmol*, vol. 117, no. 5, pp. 631–637, May 1999.
- [3] Conceição Lobo, Rui Bernardes, and José Cunha-Vaz, "Alterations of the blood-retinal barrier and retinal thickness in preclinical retinopathy in subjects with type 2 diabetes," *Arch Ophthalmol*, vol. 118, no. 10, pp. 1364–1369, October 2000.
- [4] Conceição Lobo, Rui Bernardes, José Rui Faria de Abreu, and José Cunha-Vaz, "One-year follow-up of blood-retinal barrier and retinal thickness alterations in patients with type 2 diabetes mellitus and mild nonproliferative retinopathy," *Arch Ophthalmol*, vol. 119, no. 10, pp. 1469–1474, October 2001.
- [5] Rui Bernardes, Conceição Lobo, and José Cunha-Vaz, "Multimodal macula mapping: A new approach to study diseases of the macula," *Surv Ophthalmol*, vol. 47, no. 6, pp. 580–589, November-December 2002.
- [6] George Matsopoulos, Pantelis Asvestas, Nikolaos Mouravliansky, and Konstantinos Delibasis, "Multimodal registration of retinal images using self organizing maps," *IEEE Transactions on Medical Imaging*, vol. 23, no. 12, pp. 1557–1563, December 2004.
- [7] J. Pearson, D. Hines, S. Golosman, and C. Kuglin, "Video-rate image correlation processor," in *Proceedings of SPIE: applications of Digital Image Processing*, 1977, vol. 119, pp. 197–205.
- [8] L. Rangarajan, H. Chui, and F. Bookstein, "The softassign procrustes matching algorithm," in *Information Processing in Medical Imaging*, James Duncan and Gene Gindi, Eds., pp. 29–42. Springer, 1997.
- [9] Derek Hill and Philippe Batchelor, "Registration methodology: Concepts and algorithms," in *Medical Image Registration*, Joseph Hajnal, Derek Hill, and David Hawkes, Eds., The Biomedical Engineering Series, chapter 3, pp. 39–70. CRC Press, 2001.
- [10] Barbara Zitov and Jan Flusser, "Image registration methods: A survey," *Image and Vision Computing*, vol. 21, pp. 977–1000, 2003.